ELSEVIER

Journal of Crystal Growth 211 (2000) 302–307

JOURNAL OF CRYSTAL GROWTH

www.elsevier.nl/locate/jcrysgro

Growth of Ce-doped $LiCaAlF_6$ and $LiSrAlF_6$ single crystals by the Czochralski technique under CF_4 atmosphere

Kiyoshi Shimamura[a,*], Sonia L. Baldochi[a], Na Mujilatu[a], Kenji Nakano[a], Zhenlin Liu[b], Nobuhiko Sarukura[b], Tsuguo Fukuda[a]

[a]*Institute for Materials Research, Tohoku University, 2-1-1 Katahira, Aoba-ku, Sendai 980-8577, Japan*
[b]*Institute for Molecular Science, Okazaki 444-8585, Japan*

Abstract

Ce-doped $LiCaAlF_6$ (LiCAF) and $LiSrAlF_6$ (LiSAF) single crystals were grown by the Czochralski technique. The formation of inclusions and cracks accompanying the crystal growth was investigated. The effective distribution coefficients of Ce^{3+} in LiCAF and LiSAF were determined to be 0.021 and 0.013, respectively. Ultraviolet pulse generation with an output energy of 60 mJ was obtained from a Ce : LiCAF laser.

Keywords: $LiCaAlF_6$; $LiSrAlF_6$; Crystal growth; Effective distribution coefficient; UV laser

1. Introduction

Coherent optical sources in the ultraviolet (UV) wavelength region are useful for many practical applications, such as medical procedures, semiconductor processing and remote sensing [1]. Recently, Ce-doped $LiCaAlF_6$ (Ce : LiCAF) and $LiSrAlF_6$ (Ce : LiSAF) single crystals have been reported as leading candidates for tunable all-solid-state-lasers in the UV wavelength region [2,3]. However, due to the limited size of the available crystals, it was difficult to obtain high-energy output directly from a Ce : LiCAF laser. The growth of Ce : LiCAF, especially, is known to be difficult. For the growth of this crystal, a fluorination process using gases such as HF [4] is usually performed in order to purify both raw materials and growing crystals.

We have previously reported the growth of Ce : LiCAF crystals without either the use of HF gases or the hydrofluorination of raw materials [5]. Instead, a growth chamber was evacuated to $\sim 10^{-2}$ Torr prior to growth, and a high-purity Ar (99.9999%) gas was used as a growth atmosphere. Under these conditions, a deposit of a white foreign substance was found on the surface of the grown crystals. The formation mechanism of the white substance was then investigated. In order to avoid its formation and grow high-quality crystals with higher reproducibility, several modifications such as high vacuum atmosphere prior to growth, the use of CF_4 gas instead of Ar, and a growth with a low-temperature gradient, were required [6,7].

In the present work, we describe the growth of Ce : LiCAF and Ce : LiSAF single crystals by the Czochralski (CZ) technique under modified growth

* Corresponding author. Tel.: +81-22-215-2103; fax: +81-22-215-2104.

E-mail address: shimak@lexus.imr.tohoku.ac.jp (K. Shimamura)

0022-0248/00/$ - see front matter
PII: S0022-0248(99)00789-7

conditions based on the investigations of Ref. [5]. Problems accompanying the crystal growth, such as inclusions and cracks, were investigated. High laser performance with an output energy of 60 mJ was achieved using Ce : LiCAF crystals grown in this way.

2. Experimental procedure

Crystal growth was performed in a CZ system with a resistive heater made of high-purity graphite. The starting material was prepared from commercially available AlF_3, CaF_2, SrF_2, and LiF powders of high purity (>99.99%, Rare Metallic Co., Ltd.). The composition was 1 mol% LiF and AlF_3 enriched from a stoichiometric one, in order to compensate for the vaporization of LiF and AlF_3. As dopants, CeF_3 and NaF powders of high purity (>99.99%, Rare Metallic Co., Ltd.) were used. Na^+ was co-doped with Ce^{3+} in order to maintain the charge neutrality. The concentration of Ce^{3+} and Na^+ in the starting material was 1 mol%. The starting material was placed in a Pt crucible. Growth orientation was controlled by using *a*-axis oriented Cr^{3+}-doped LiCAF and LiSAF seed crystals. The pulling rate was 1 mm/h and the rotation rate was 10 rpm.

Vacuum treatment was performed prior to growth. The system was heated from room temperature to 700°C for a period of 12 h under vacuum ($\approx 10^{-5}$ Torr). Both rotary and diffusion pumps were used to achieve $\approx 10^{-5}$ Torr and effectively eliminate water and oxygen from the growth chamber and the starting material. Subsequently, high-purity CF_4 gas (99.9999%) was slowly introduced into the furnace. Thereafter, the starting material was melted at approximately 820°C.

The determination of lattice parameters and the phase identification were performed by the X-ray powder diffraction method (XRD). Chemical composition was determined by the induced coupled plasma method. Absorption spectra in infrared (IR) wavelength region were measured by FT–IR with high resolution. To measure the transmission edge in the vacuum–ultra-violet (VUV) wavelength region at room temperature, an experiment was performed at the beam line BL1B of the Ultraviolet Synchrotron Orbital Radiation Facility (UVSOR) using a 1-m focal-length Seya-Namioka monochromator [8]. The transmission at wavelengths from 100 to 200 nm was detected by a photomultiplier (Hamamatsu R105).

3. Results and discussion

Fig. 1 shows as-grown Ce : LiCAF and Ce : LiSAF single crystals with dimensions of 18 mm in diameter and 60 mm in length. Cracks, bubbles and inclusions were not observed. Under the modified growth conditions, foreign substances on the surface of the grown crystal, as observed in Ref. [5], were not formed. However, Ce : LiSAF showed a tendency to crack perpendicular to the growth axis after several days. On the contrary, Ce : LiCAF did not show cracks at any time.

Fig. 2 shows the dependence of the lattice parameters *a* and *c* on the solidification fraction. Along the growth axis, both *a* and *c* of Ce : LiCAF and Ce : LiSAF were almost constant. Fig. 3 shows the distribution of Ce^{3+} concentration along the growth axis. The effective distribution coefficient (k_{eff}) of Ce^{3+} in LiCAF and LiSAF has been determined to be 0.021 and 0.013, respectively, by the following equation [9]:

$$\frac{C_{\mathrm{S}}}{C_0} = k_{\mathrm{eff}}(1-g)^{k_{\mathrm{eff}}-1}. \tag{1}$$

Solid and dotted lines in Fig. 3 were obtained using Eq. (1). The k_{eff} of Ce^{3+} in LiCAF was larger than in LiSAF. This is because the ionic radius of Ce^{3+} under six-fold coordination (1.01 Å) is closer to that of Ca^{2+} (1.00 Å) than to that of Sr^{2+} (1.18 Å) [10], the ions thought to be replaced by Ce^{3+} [5]. Although the concentration of Ce^{3+} showed a tendency to increase slightly with solidification fraction, this change did not affect the lattice parameter because of the small value of k_{eff}.

Fig. 4 shows an as-grown Ce : LiCAF single crystal of 1″ diameter, free from cracks and inclusions. When crystals of this diameter were grown, the following two problems, not observed for crystals of 18 mm diameter, appeared: formation of inclusions, and cracks accompanied by the

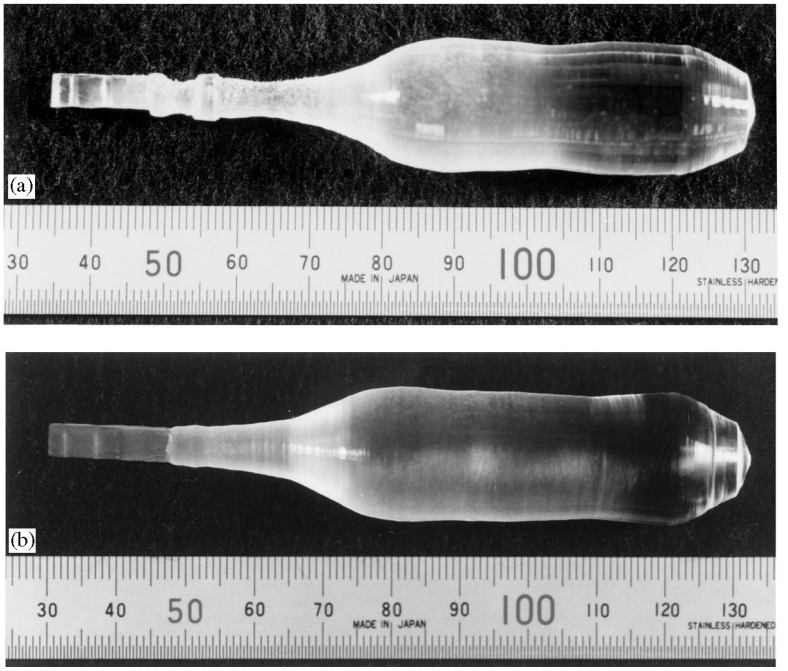

Fig. 1. As-grown Ce-doped (a) $LiCaAlF_6$ and (b) $LiSrAlF_6$ single crystals of 18 mm diameter pulled along the *a*-axis.

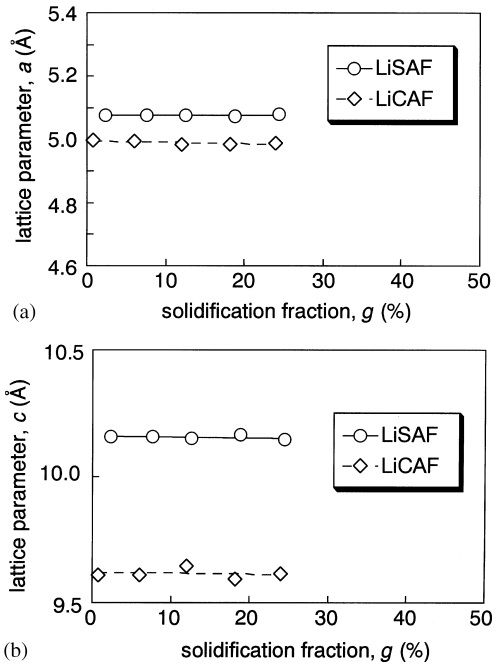

Fig. 2. Dependence of the lattice parameters on solidification fraction, measured for Ce-doped $LiCaAlF_6$ and $LiSrAlF_6$ single crystals. (a) *a*- and (b) *c*-axis, respectively.

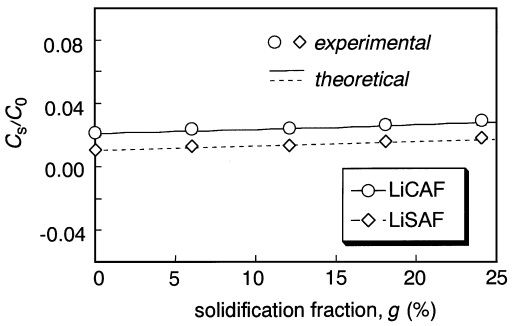

Fig. 3. Concentration dependence of Ce^{3+} on solidification fraction, measured for Ce-doped $LiCaAlF_6$ and $LiSrAlF_6$ single crystals. C_0 and C_s are the initial concentration and the concentration at each solidification fraction, respectively.

formation of an impurity phase at the bottom of the crystal.

Fig. 5 shows a polished wafer cut parallel to the growth axis. Many inclusions are distributed throughout the crystal. It should be noted that the formation of these inclusions was related to a change of the crystal diameter, for example at the shoulder part of the crystal. Once they appeared at

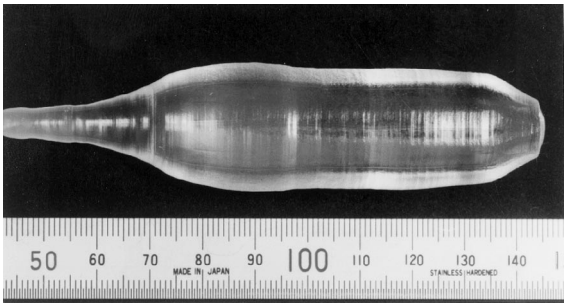

Fig. 4. As-grown Ce-doped $LiCaAlF_6$ single crystal 1″ in diameter.

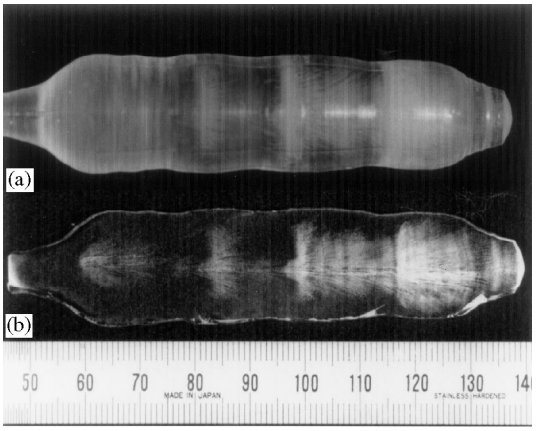

Fig. 5. Ce-doped $LiCaAlF_6$ crystal with inclusions: (a) as-grown crystal and (b) wafer cut parallel to the growth axis.

the shoulder part, they did not disappear during crystal growth. In order to avoid these inclusions, the diameter at the shoulder part had to be controlled precisely and extended smoothly, without rapid change of the diameter. Fig. 6 shows absorption spectra for the wafer shown in Fig. 5b, in regions with and without inclusions. Although the absorption spectrum for the inclusion free region did not show any absorption peaks, that of the region with inclusions had one small absorption peak around 3600 cm^{-1}. Since this peak indicates the existence of OH^- [1], it is thought that H_2O-based impurities were present in the inclusions.

Fig. 7 shows an as-grown crystal with one large crack along the growth axis and a white substance at the bottom of the crystal. This large, flat crack appeared during cooling after growth, in cases when white material was present. This white substance is usually formed when the solidification fraction exceeded 70%. The XRD analysis showed that the white substance was composed of LiCAF and CaF_2 phases. This is because the melt composition shifted in the CaF_2-enriched direction during growth, since the vaporization pressure of LiF and AlF_3 is very high [11]. CeF_3 and NaF might have accumulated in the residual melt due to the small k_{eff}. In order to avoid formation of this white substance, crystal growth was terminated at the solidification fraction 60%, as for the crystal shown in Fig. 4. For further improvement, optimization of melt composition should be carried out.

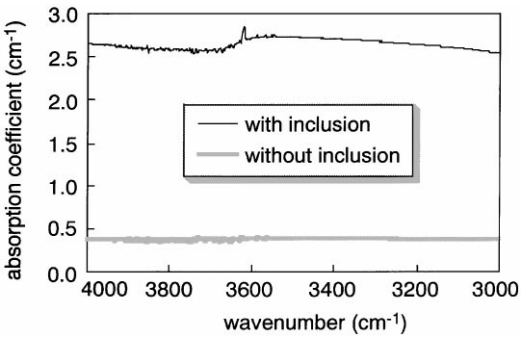

Fig. 6. Infrared absorption spectra of the crystal shown in Fig. 5.

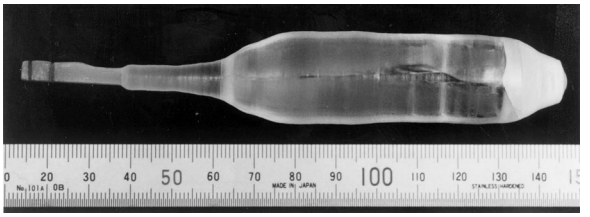

Fig. 7. As-grown Ce-doped $LiCaAlF_6$ single crystal with white substance at the bottom of the crystal and a large crack parallel to the growth axis.

Fig. 8 shows the transmission edge of the LiCAF and LiSAF single crystals grown in this work. The transmission edge of LiCAF was measured to be at 112 nm and that of LiSAF 116 nm, the shortest reported to our knowledge. This difference may explain the solarization-free nature of Ce : LiCAF compared with Ce : LiSAF. The absorption at around 125 nm might be due to a color center or impurity. Therefore, after the crystal quality is improved, this absorption should disappear. These

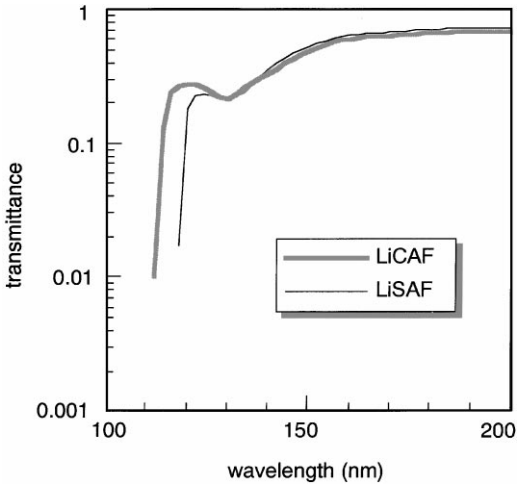

Fig. 8. Transmission spectra of un-doped $LiCaAlF_6$ and $LiSrAlF_6$ single crystals in the vacuum–ultra violet wavelength region.

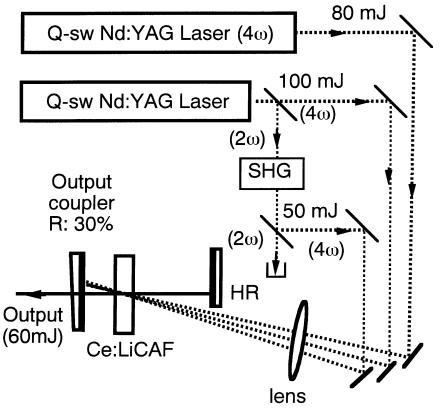

Fig. 9. Experimental setup of a high-energy Ce : $LiCaAlF_6$ laser.

transmission characteristics of LiCAF and LiSAF show their high potential as optical window materials in the UV and VUV wavelength region.

The problems of commonly used optical materials for the UV and VUV region, such as LiF, are the limitation of transmission wavelength, solarization of the material under irradiation by high-power UV light, and the difficulty of material processing and polishing due to the cleavage or hydroscopic nature of the material. LiCAF does not have these problems, and therefore will be a suitable optical material for the UV and VUV region, becoming much more important in the next generation of lithographic technology.

We have already demonstrated an output energy of 30 mJ from a UV solid-state Ce : LiCAF laser that operated at 290 nm at a repetition rate of 10 Hz [5,12]. In order to obtain higher output energy, we increased the pumping energy. The laser resonator was formed by a flat high reflector and a flat output coupler with 30% reflectivity, separated by 4 cm as shown in Fig. 9. The large Ce : LiCAF crystal (aperture 15 mm × 10 mm) was located midway between the two cavity end mirrors. The fourth harmonics of two simultaneously Q-switched Nd : YAG lasers were used as pumping sources. The three pump beams were focused with a 40 cm focal length lens to produce a spot size of 6 mm at the surface of the Ce : LiCAF crystal. We obtained 60 mJ at 10 Hz, to our knowledge the highest performance so far reported for Ce : LiCAF.

4. Summary

Ce : LiCAF and Ce : LiSAF single crystals of 18 mm diameter were grown by the CZ technique under CF_4 atmosphere. Ce : LiSAF showed a tendency to crack after growth. The lattice parameters of Ce : LiCAF and Ce : LiSAF were almost constant along the growth axis. The effective distribution coefficients of Ce^{3+} in LiCAF and LiSAF were determined to be 0.021 and 0.013, respectively. Under the same growth conditions, Ce : LiCAF single crystals of 25 mm diameter (1″) were also grown up to a solidification fraction of 60%. Although numerous inclusions appeared during growth, precise diameter control prevented their formation. Un-doped LiCAF and LiSAF single crystals showed transmission edges at 112 and 116 nm, respectively. These characteristics indicate the high potential of these crystals as optical window materials. Laser output energy of 60 mJ was obtained using the grown crystals. This demonstrates that Ce : LiCAF is a promising material for high-energy UV pulse generation.

Acknowledgements

The authors would like to express sincere thanks to Associate Professor S. Durbin of the Institute for

Materials Research, Tohoku University, for critical reading of the manuscript and fruitful discussions. The authors are also indebted to Dr. T. Shoji of the Institute for Materials Research, Tohoku University, for help in carrying out the chemical composition analysis.

References

[1] N. Sarukura, M.A. Dubinskii, Z. Liu, V.V. Semashko, A.K. Naumov, S.L. Korableva, R.Y. Abdulsabirov, K. Edamatsu, Y. Suzuki, T. Itoh, Y. Segawa, IEEE J. Selected Topics Quantum Electron. 1 (1995) 792.
[2] M.A. Dubinskii, V.V. Semashko, A.K. Naumov, R.Y. Abdulsabirov, S.L. Korableva, Laser Phys. 3 (1993) 216.
[3] C.D. Marshall, S.A. Payne, J.A. Speth, W.F. Krupke, G.J. Quarles, V. Castillo, B.H.T. Chai, J. Opt. Soc. Am. B 11 (1994) 2054.
[4] R.F. Belt, R. Uhrin, J. Crystal Growth 109 (1991) 340.
[5] K. Shimamura, Na Mujilatu, K. Nakano, S.L. Baldochi, Z. Liu, H. Ohtake, N. Sarukura, T. Fukuda, J. Crystal Growth 197 (1999) 896.
[6] S.L. Baldochi, K. Shimamura, K. Nakano, Na Mujilatu, T. Fukuda, J. Crystal Growth 200 (1999) 521.
[7] S. L. Baldochi, K. Shimamura, K. Nakano, Na Mujilatu, T. Fukuda, J. Crystal Growth 205 (1999) 537.
[8] M. Kamada, H. Hama, T. Kinoshita, N. Kosugi, J. Synchrotron Rad. 5 (1998) 1166.
[9] J.S. Shah, in: B.R. Pamplin (Ed.), Crystal Growth and Characterization, Vol. 6, Pergamon Press, Oxford, 1975, p. 114 (Chapter 4).
[10] R.D. Shannon, Acta Crystallogr. A 32 (1976) 751.
[11] D. Klimm, P. Reiche, Proceedings of International Symposium on Laser and Nonlinear Optical Materials, 3–5 November 1997, p. 284.
[12] Z. Liu, S. Izumida, H. Ohtake, N. Sarukura, K. Shimamura, Na Mujilatu, S.L. Baldochi, T. Fukuda, Jpn. J. Appl. Phys. 37 (1998) L1318.